



ehponline.org

ENVIRONMENTAL HEALTH PERSPECTIVES

Coplanar Polychlorinated Biphenyls Impair Glucose Homeostasis in Lean C57BL/6 Mice and Mitigate Beneficial Effects of Weight Loss on Glucose Homeostasis in Obese Mice

Nicki A. Baker, Michael Karounos, Victoria English, Jun Fang, Yinan Wei, Arnold Stromberg, Manjula Sunkara, Andrew J. Morris, Hollie I. Swanson, Lisa A. Cassis

<http://dx.doi.org/10.1289/ehp.1205421>

Online 24 October 2012



NIEHS

National Institute of
Environmental Health Sciences

National Institutes of Health
U.S. Department of Health and Human Services

Coplanar Polychlorinated Biphenyls Impair Glucose Homeostasis in Lean C57BL/6 Mice and Mitigate Beneficial Effects of Weight Loss on Glucose Homeostasis in Obese Mice

Nicki A. Baker,¹ Michael Karounos,¹ Victoria English,¹ Jun Fang,² Yinan Wei,² Arnold Stromberg,³ Manjula Sunkara,⁴ Andrew J. Morris,⁴ Hollie I. Swanson,⁵ Lisa A. Cassis^{1,5}

¹Graduate Center for Nutritional Sciences, ²Department of Chemistry, ³Department of Statistics, ⁴Division of Cardiovascular Medicine, and ⁵Department of Molecular and Biomedical Pharmacology, University of Kentucky, Lexington, Kentucky, USA

Corresponding author:

Lisa A. Cassis, PhD
Professor and Chair
Graduate Center for Nutritional Sciences
University of Kentucky
Room 521b, Wethington Building
900 S. Limestone
Lexington, KY 40536-0200
Phone: 859-323-4933 ext 81400
Fax: 858-257-3646
e-mail: lcassis@uky.edu

Running title: Coplanar PCBs impair glucose homeostasis

Key words: adipose, diabetes, glucose tolerance, polychlorinated biphenyl

Acknowledgements: This work was supported by grant P42ES007380 from the National Institutes of Environmental Health Sciences, National Institutes of Health, and through core services supported by a grant from the National Institute of General Medical Sciences (8 P20 GM103527-05).

The author's freedom to design, conduct, interpret and publish research is not compromised by any controlling sponsor as a condition of review or publication. The authors declare they have no actual or pending competing financial interest.

Abbreviations:

AhR – Aryl hydrocarbon receptor

AUC – Area under the curve

IL6 – Interleukin 6

LF – Low fat

HF – High fat

PCB – Polychlorinated biphenyl

ROS – Reactive oxygen species

T2D – Type 2 diabetes

TNF- α – Tumor necrosis factor-alpha

Abstract

BACKGROUND: Previous studies demonstrated that coplanar polychlorinated biphenyls (PCBs) promote proinflammatory gene expression in adipocytes. PCBs are highly lipophilic and accumulate in adipose, a site of insulin resistance in type 2 diabetics.

OBJECTIVES: To investigate *in vitro* and *in vivo* effects of coplanar PCBs on adipose expression of tumor necrosis factor alpha (TNF- α) and glucose and insulin homeostasis in lean and obese mice.

METHODS: Male C57BL/6 mice were fed a low fat (LF) diet and administered vehicle, PCB-77 or 126. Glucose and insulin tolerance, as well as TNF- α levels were quantified in liver, muscle and adipose. Mice administered vehicle or PCB-77 were fed a high fat (HF) diet for 16 weeks, and then switched to a LF diet to induce weight loss. Glucose and insulin tolerance and adipose TNF- α expression were quantified. *In vitro* and *in vivo* studies quantified aryl hydrocarbon receptor (AhR)-dependent effects of PCB-77 on parameters of glucose homeostasis.

RESULTS: Coplanar PCBs resulted in sustained impairment of glucose and insulin tolerance in LF-fed mice. PCB-77 increased TNF- α expression in adipose, but not liver or muscle. PCB-77 levels were strikingly higher in adipose than liver or serum. Antagonism of AhR abolished *in vitro* and *in vivo* effects of PCB-77. In obese mice, PCB-77 had no effect on glucose homeostasis, but impaired glucose homeostasis upon weight loss.

CONCLUSIONS: Coplanar PCBs impair glucose homeostasis in lean mice and in obese mice upon weight loss. Adipose-specific elevations in TNF- α expression by PCBs may contribute to impaired glucose homeostasis.

Introduction

Type 2 diabetes (T2D) affects 300 million people with an anticipated doubling of diabetes prevalence world-wide over the next 20 years (Shaw et al. 2010). Recent epidemiological studies suggest that exposure to low concentrations of PCBs that are similar to current exposure levels in humans increases diabetes risk (Lee et al. 2010). Multiple cross-sectional analyses of NHANES cohorts from years 1999-2006 demonstrated that PCB-170 concentrations in urine or blood had an adjusted odds ratio of 4.5 for T2D, predicting up to 15% risk (Patel et al. 2010). Remarkably, this increased risk appeared in individuals who are not overweight or obese (Carpenter 2008). Similar observations linking PCB exposures to T2D have been reported in other populations (Codru et al. 2007; Wang et al. 2008). Recently, a significant association between elevated PCB levels and diabetes was found in the Anniston Community Health Survey (Silverstone et al. 2012). Collectively, accumulating evidence supports a link between PCB exposure levels and the development of diabetes, but mechanisms linking PCBs to diabetes are largely unknown.

Due to their lipophilicity, PCBs accumulate in lipid stores of adipose tissue (Kodavanti et al. 1998), suggesting that adipocytes experience continuous low-grade exposures to PCBs. Extension of these findings to the setting of obesity suggests that the total body burden of PCBs would increase in obese subjects due to the inherent lipophilicity of these compounds. Recent studies demonstrated an inverse relationship between serum levels of several PCBs and body mass index, suggesting sequestration of PCBs in adipose tissue is enhanced with obesity (Dirinck et al. 2011). It is unclear whether enhanced sequestration in adipose tissue with obesity limits effects of PCBs systemically. Given the epidemic of obesity and T2D in the US, a large

percentage of the population strives to lose weight. Weight loss, through dietary restriction or increased physical activity, typically reduces adipose tissue mass through liberation of lipid stores (Walford et al. 1999). In obese subjects undergoing a weight-loss program, plasma concentrations of organochlorines increased and significantly correlated to reductions in body mass index (Lim et al. 2011). Further, plasma concentrations of 13 out of 17 organochlorines in serum increased in obese subjects experiencing weight loss (Pelletier et al. 2002). The consequences of increased liberation of PCBs following weight loss in obese subjects on indices of T2D are unknown.

Previous studies in our laboratory demonstrated that low concentrations of coplanar PCB-77, a ligand of the aryl hydrocarbon receptor (AhR), promoted adipocyte differentiation and the production of proinflammatory adipokines (Arsenescu et al. 2008). Recent studies demonstrated that PCB-126, a coplanar AhR ligand, promoted inflammatory gene expression in human preadipocytes and adipocytes, and also increased inflammatory gene expression in adipose tissue from wild type, but not AhR deficient mice (Kim et al. 2012). Amongst several inflammatory cytokines stimulated by coplanar PCBs in adipocytes (Arsenescu et al. 2008; Kim et al. 2012), tumor necrosis alpha (TNF- α) is a recognized contributor to insulin resistance (Hotamisligil et al. 1996; Ventre et al. 1997). TNF- α promotes insulin resistance through downstream alternative phosphorylation of the insulin receptor (IR) docking protein, insulin receptor substrate-1 (IRS-1) (Peraldi et al. 1996), which prevents phosphorylation of protein kinase B (Akt) (Thong et al. 2005) and impairs transport of glucose transporter type 4 vesicles in skeletal muscle and adipose to the plasma membrane (Peraldi and Spiegelman 1998). TNF- α can indirectly contribute to

adipocyte insulin resistance by promoting lipolysis (Cawthorn and Sethi 2008) and/or inhibiting differentiation (Torti et al. 1989).

In this study, we defined dose-dependent effects of coplanar PCBs on glucose homeostasis in lean mice. To define mechanisms for PCB-induced impairment of glucose and insulin tolerance, we quantified expression levels of TNF- α in organs contributing to insulin resistance. Moreover, we defined the sustainability of PCB-induced impairment of glucose homeostasis in lean mice in reference to organ and serum concentrations of PCBs. To delineate the role of AhR in effects of PCBs, we examined *in vitro* and *in vivo* effects of an AhR antagonist on parameters of glucose homeostasis. Since T2D is frequently associated with obesity, we examined effects of a coplanar PCB on glucose homeostasis in obese mice. In addition, since PCBs redistribute from adipose to the circulation with weight loss, we determined effects of previous PCB exposures in obese mice on glucose homeostasis when obese mice experienced weight loss.

Materials and Methods

Chemical Procurement. 3,3',4,4'-tetrachlorobiphenyl (PCB-77) and 3,3',4,4',5-pentachlorobiphenyl (PCB-126) were purchased from AccuStandard Inc. (New Haven, CT). CH223191 was a generous gift from Dr. Hollie Swanson (University of Kentucky, Lexington, KY).

Animal treatments and sample collection. All experimental procedures met the approval of the Animal Care and Use Committee of the University of Kentucky. We treated animals humanely and with regard for alleviation and suffering. Male, C57BL/6 mice (2 months of age; The Jackson Laboratory, Bar Harbor, ME) were given *ad libitum* access to food and water and housed in a pathogen-free environment. Initial studies examined glucose and insulin tolerance in mice administered vehicle (tocopherol stripped safflower oil), PCB-77 (2.5, 50, 248 mg/kg, by oral gavage given as 2 separate doses over 2 weeks; n = 10 mice/group) or PCB-126 (0.3, 1.6, or 3.3 mg/kg by oral gavage; n = 10 mice/group). We fed mice in dose response studies a low fat diet (LF, 10% kcal as fat; Research Diets, Inc., New Brunswick, NJ). To define the sustainability of PCB effects, we performed temporal studies in mice fed a LF diet. Mice were administered vehicle or PCB77 (50 mg/kg by oral gavage) in week 1 and 2, and then for mice examined at later time points (12 weeks), a second set of oral gavages was administered at weeks 9 and 10. Mice in each treatment group (vehicle, PCB77) were examined at weeks 2, 4 or 12 after onset of LF diet feeding. Body weights were quantified weekly in all studies. At study endpoint, mice were anesthetized (ketamine/xylazine, 10/100 mg/kg, ip) for exsanguination and tissue harvest (liver, soleus muscle, visceral adipose). A sub-set of mice (n = 5/group) in each

treatment group were administered insulin (10 U/kg(Kienesberger et al. 2009)) 10 minutes prior to exsanguination to elicit insulin signaling pathways.

For studies examining obesity/weight loss, male C57BL/6 mice (2 months of age; n = 10/group) were fed a high fat diet (HF, 60% kcal as fat; Research Diets, Inc., New Brunswick, NJ) for 12 weeks and administered vehicle or PCB-77 (50 mg/kg by oral gavage) at weeks 1, 2, 9 and 10. Body weight was quantified weekly. At 12 weeks of HF feeding, a sub-set of mice (n = 3/group) were anesthetized for exsanguination and tissue harvest. The remaining mice in each treatment group were then fed the LF diet for 4 weeks to induce weight loss.

To determine if *in vivo* effects were AhR-mediated, male C57BL/6 mice (2 months old; n = 7/group) were fed the LF diet and orally gavaged with vehicle or 2-methyl-2H-pyrazole-3-carboxylic acid (10 mg/kg/day; 2-methyl-4-o-tolylazo-phenyl-amide, CH-233191) (Kim et al. 2006; Choi et al. 2012) for one week prior to administration of vehicle or PCB77 and through the remainder of the study. After 1 week of pretreatment with CH-233191, mice were administered vehicle or PCB-77 (50 mg/kg by oral gavage, given as two separate doses in week 1,2). Within 48 hours after the last dose of vehicle/PCB-77, glucose and insulin tolerance tests were performed.

Glucose (GTT) and insulin tolerance tests (ITT). Mice were fasted for 6 or 4 hours prior to quantification of GTT or ITT, respectively. Blood glucose concentrations were measured via the tail vein using a hand held glucometer (Freedom Freestyle Lite, Abbott Laboratories, Abbott Park, IL). Mice were injected with D-glucose (20% in saline, ip) or human insulin (0.0125

uM/gm body weight, Novolin, ip) and blood glucose was quantified at 0 - 120 minutes. Total area under the curve (AUC, arbitrary units), which is obtained without the presence of a baseline, calculates the area below the observed concentrations and in comparison studies was reported to compare favorably to the positive incremental area method for statistical analyses of glucose tolerance data (Cardoso et al. 2011).

Quantification of PCBs. Frozen tissue samples (epididymal adipose, liver, skeletal muscle) or mouse sera were spiked with surrogate standards (100 μ l of 0.35 ng/ μ l PCB-166 in isooctane). After the addition of 1.0 g of diatomaceous earth, the mixture was grained into fine powders and transferred into an extraction cell filled with Ottawa Sands. Extraction with hexane (30 mL) was performed using an ASE 200 accelerated solvent extractor (Dionex Corporation, Sunnyvale, CA). Lipids were removed by the addition of an equal volume of concentrated sulfuric acid. For adipose samples containing high lipid content, hexane extracts were subjected to de-lipidation by passing over a Florisil SPE column following the manufacturer's instructions before acid treatment. The hexane layer containing PCBs was collected and concentrated to (2 mLs) using a Heidolph Synthesis1 evaporator (Heidolph, Schwabach, Germany) and then to 100 μ l using a gentle stream of nitrogen. Then, 10 μ L of 1.0 ng/ μ L of internal standard PCB-209 was added.

Gas chromatographic analysis was performed with a GC-MS system (Agilent GC 6890N, auto sampler G2913A, MS 5975 detector) (Agilent Technologies, Santa Clara, CA) using a HP-5MS 5% Phenyl Methyl Siloxane (30m length, 0.25 mm internal diameter, 0.25 μ m film thickness) column. The column temperature was held at 60°C for 1 min, then increased to 200 °C at a rate of 40 °C /min followed by a rate of 4 °C /min to 280 °C where it was held for 5.5 min.

The injector temperature was 250 °C. The carrier gas was ultra pure helium, and the makeup gas was nitrogen. PCBs were identified on the basis of their retention times relative to standards. Quantification was achieved based on calibration curves obtained using PCB standards. The recovery efficiency was calculated from the surrogates and the sample weight.

Quantification of plasma components. Plasma insulin concentrations were quantified using a commercial ELISA (Crystal Chem, Downers Grove, IL). Plasma TNF- α and IL-6 concentrations were quantified using a commercial Milliplex MAP Mouse Serum Adipokine kit (Millipore, St. Charles, MO).

Extraction of RNA and quantification of mRNA abundance using real-time polymerase chain reaction (PCR). Total RNA was extracted from tissues using the SV Total RNA Isolation System kit (Promega Corporation, Madison, WI) (Arsenescu et al. 2008). RNA concentrations were quantified and cDNA was synthesized from total and amplified using an iCycler (Bio-Rad, Hercules, CA) with the Perfecta SYBR Green Fastmix for iQ (20 μ L; Quanta Biosciences, Gaithersburg, MD). Using the difference from 18S rRNA (reference gene) and the delta Ct method, the relative quantification of gene expression was calculated. The PCR reaction was: 94°C for 5 minutes, 40 cycles at 94°C for 15 seconds, 58°C or 64°C (based on tested primer efficiency) for 40 seconds, 72°C for 10 minutes, and 100 cycles from 95°C to 45.5°C for 10 seconds. Primer sequences are as follows: 18S, Forward 5'AGTCGGCATCGTTTATGGTC-3', Reverse 5'-CGAAAGCATTTGCCAAGAAT-3'; CYP1A1, Forward 5'AGTCAATCTGAGCAATGAGTTTGG-3', Reverse 5'-GGCATCCAGGGAAGAGTTAGG-3'; F4/80, Forward 5'-CTTTGGCTATGGGCTTCCAGTC-3', Reverse 5'-

GCAAGGAGGACAGAGTTTATCGTG-3'; TNF- α , Forward 5'-
 CCCACTCTGACCCCTTTACTC-3', Reverse 5'- TCACTGTCCCAGCATCTTGT-3'.

Western blotting. Tissues (liver, soleus muscle, epididymal adipose tissue) were homogenized in mammalian protein extraction reagent (M-PER) (Thermo Scientific, Rockford, IL), sonicated, and centrifuged, and supernatants were used to quantify protein. Proteins were resolved on 4-15% precast polyacrylamide gels (Bio-Rad Laboratories, Hercules, CA), transferred onto a PVDF transfer membrane (GE Healthcare, Buckinghamshire, UK), and non-specific proteins blocked for 1 hour at room temperature (5% nonfat milk in PBS-0.1% Tween-20, 60 min, 25°C). Membranes were then incubated with primary antibody (anti-TNF α , 1:1000; rabbit, Novus Biologicals, Littleton, CO; β -actin, 1:5000; mouse; Cell Signaling, Beverly, MA) in diluted PBS overnight at 4°C. After stripping primary antibody, secondary goat anti-rabbit IgG HRP-linked antibody (1:5000; Cell Signaling) was incubated with membranes for 1 hour at room temperature. Protein levels were quantified using Kodak Molecular Imaging Software (Carestream Health, Inc., Rochester, NY).

Cell culture. 3T3-L1 mouse preadipocytes, obtained from American Type Culture Collection (Manassas, VA) were cultured as described previously (Arsenescu et al. 2008). Differentiation was induced by incubating cells for 2 days with media containing insulin (0.1 μ M; Sigma, St. Louis, MO), dexamethasone (1 μ M; Sigma), and isobutylmethyl xanthine (0.5 mM, IBMX; Sigma), and then insulin for 1 additional day. Assays (n = 3/group) were performed on duplicate wells of cells. Differentiated adipocytes (day 8) were incubated with vehicle [0.03% dimethyl sulfoxide (DMSO)] or PCB-77 (3.4 μ M; 24 hrs) (Arsenescu et al. 2008). The concentration of

PCB-77 was based on the maximum serum level of PCB-77 (0.84 ug/g, converted to $\approx 3 \mu\text{M}$) measured in experimental mice, as described above, at week 2 after administration of PCB-77 (50 mg/kg). Adipocytes from each treatment group were incubated with the AhR antagonist, α -naphthoflavone (NF) (20 μM) for 30 min before the addition of vehicle or PCB-77 (3.4 μM).

Statistical analysis. Data are represented as mean \pm SEM. Total AUC and mRNA abundance data were log transformed. A one-way ANOVA was used to define treatment effects of different doses of PCBs and for studies using CH223191 (SigmaPlot, Version 12.0, Systat Software Inc., Chicago, IL). In studies examining sustainability of PCB effects in lean mice, total AUC was analyzed using two-way ANOVA with Holm-Sidak method for post-hoc analysis. In studies utilizing obese mice and mice undergoing weight loss, a mixed model analysis of repeated measures, total AUC was analyzed using two-way ANOVA (JMP, Version 10, SAS Institute Inc., Cary, NC). Statistical significance was defined as $P < 0.05$.

Results

Coplanar PCBs dose-dependently impair glucose and insulin tolerance in LF-fed mice in an AhR-dependent manner. We defined dose-dependent effects of two coplanar PCBs (PCB-77 or PCB-126) that are prevalent in the environment (McFarland and Clarke 1989) and/or linked to T2D (Carpenter 2008; Everett et al. 2007) on glucose and insulin tolerance in LF-fed mice. At 48 hours after the final dose, PCB-77 (50 mg/kg) or PCB-126 (1.6 mg/kg) resulted in a significant increase in blood glucose concentrations following a bolus of administered glucose compared to controls (Fig. 1A,B, respectively; $P < 0.05$). Total AUC for blood glucose

concentrations was significantly increased in mice administered these doses of PCB-77 or PCB-126 (Fig. 1C,D, respectively; $P < 0.05$). Similarly, blood glucose concentrations in response to insulin administration were significantly increased in mice administered PCB-77 (50 mg/kg) or PCB-126 (3.3 mg/kg) (Supplemental Material, Figure S1A,B, respectively; $P < 0.05$), resulting in a significant increase in total AUC (Figure S1C,D, respectively; $P < 0.05$). Fasting plasma insulin concentrations were similar in mice administered vehicle or PCB77 (vehicle, 0.18 ± 0.10 ; PCB-77, 0.19 ± 0.09 ng/ml; $P > 0.05$). Based on a higher prevalence of PCB-77 compared to PCB-126 in food (Hansen, 1998), we used PCB-77 in continued studies examining mechanisms of glucose and insulin intolerance.

To determine if *in vivo* effects of PCB-77 are AhR-mediated, we defined effects of CH-223191, an AhR antagonist, on PCB-77-induced impairment of glucose and insulin tolerance in LF-fed mice. Administration of PCB-77 significantly impaired glucose and insulin tolerance compared to mice administered vehicle, and these effects of PCB-77 were abolished in mice administered CH-223191 (Supplemental Material, Figure S2; $P < 0.05$).

PCB-77 results in sustained impairment of glucose and insulin tolerance in LF-fed mice. To define the duration of PCB-induced impairment of glucose tolerance, we administered vehicle or PCB-77 (50 mg/kg) to LF-fed (12 weeks) male C57BL/6 mice in 2 doses during weeks 1 and 2, and then administered a second set of 2 doses in weeks 9 and 10 of LF feeding. Body weight was not significantly different in mice administered vehicle or PCB-77 (12 weeks: Vehicle, 27 ± 1 , PCB-77, 28 ± 1 gm, $P > 0.05$). Glucose tolerance was significantly impaired in mice administered PCB-77 compared to controls from weeks 2 – 12 of LF feeding (Supplemental

Material, Figure S3A). Insulin tolerance was significantly impaired in mice administered PCB-77 compared to controls on weeks 2 and 4 (Supplemental Material, Figure S3B).

Due to their lipophilicity, PCBs accumulate in adipose tissue (Kodavanti et al. 1998). We quantified levels of PCB-77 in retroperitoneal white adipose (RPF), liver, skeletal muscle and serum following administration of PCB-77. PCB-77 levels were undetectable in tissues or serum from mice administered vehicle; additionally, PCB-77 was not detected in skeletal muscle from either treatment group. At week 2, PCB-77 levels in RPF were 10- and 384-fold higher than in liver or serum, respectively (192 ± 36 , 19 ± 1 , 0.5 ± 0.2 PCB-77 $\mu\text{g/g}$, respectively). At week 3, PCB-77 levels in RPF were decreased (by 53%) compared to week 2 (91 ± 37 vs 192 ± 36 PCB-77 $\mu\text{g/g}$, respectively), and were markedly decreased by weeks 4 and 12.

Previous studies demonstrated that PCB-77 increased TNF- α mRNA abundance in 3T3-L1 adipocytes (Arsenescu et al. 2008). Thus, we contrasted effects of PCB-77 on TNF- α expression in adipose compared to liver and skeletal muscle. As evidence of AhR activation by PCB-77, mRNA abundance of CYP1A1, an AhR target gene (Denison and Nagy 2003), was significantly increased in adipose tissue from mice administered PCB-77 compared to controls (Supplemental Material, Figure S4A). By comparison, CYP1A1 mRNA abundance was significantly increased in livers of mice administered PCB-77 compared to controls at week 2, but not at later time points (Supplemental Material, Figure S4B). While adipose mRNA expression of TNF- α did not reach statistically significant levels in PCB-77 treated mice (Supplemental Material, Figure S5A), TNF- α protein was significantly increased by PCB-77 at week 4 (Figure 2; $P < 0.05$). Plasma concentrations of TNF- α were significantly increased in

mice administered PCB-77 compared to controls (Supplemental Material, Figure S6A; $P < 0.05$). Plasma concentrations of interleukin-6 (IL6) were significantly increased (week 12) in mice administered PCB-77 compared to controls (Supplemental Material, Figure S6B; $P < 0.05$).

Infiltration of macrophages into adipose tissue has been suggested as a mechanism contributing to low grade inflammation from obesity and the development of insulin resistance (Harford et al. 2011). Adipose tissue from mice administered PCB-77 exhibited statistically similar mRNA abundance of the macrophage marker F4/80 compared to controls (Supplemental Material, Figure S5).

Effects of PCB-77 to promote glucose and insulin intolerance are lost in mice with diet-induced obesity, but manifest when obese mice lose weight. Obesity is associated with the development of insulin resistance in T2D (DeFronzo 2004). Moreover, obesity increases the total body burden of lipophilic PCBs (Kim et al. 2011). Thus, we defined effects of PCB-77 on glucose and insulin tolerance in mice fed a HF diet for 12 weeks (weight gain phase). In addition, we defined effects of PCB-77 on glucose and insulin tolerance in HF-fed obese mice (12 weeks) made to lose weight for 4 weeks (by switching to LF diet, weight loss phase). During the weight gain phase, administration of PCB-77 had no significant effect on body weight in mice fed a LF or HF diet compared to controls (Supplemental Material, Figure S7A). Surprisingly, administration of PCB-77 had no effect on glucose or insulin tolerance in HF-fed mice (weeks 4 or 12) compared to controls (Figure 3; weight gain phase). Moreover, mRNA abundance of TNF- α in adipose tissue was not significantly different in mice administered PCB-77 compared to controls (Supplemental Material, Figure S8). Adipose tissue levels of PCB-77 (1.8 ± 0.5 ug/tissue wet

weight) in HF-fed mice (12 weeks) were 2-fold greater than those observed in adipose tissue from LF-fed mice (12 weeks).

Previous studies demonstrated that plasma concentrations of PCBs increased in obese subjects experiencing weight loss (Chevrier et al. 2000). Thus, we defined effects of PCB-77, administered during the weight gain phase of HF feeding, on glucose homeostasis during weight loss. Administration of PCB-77 during the weight gain phase had no effect on body weight reductions induced by weight loss (Supplemental Material, Figure S7). Glucose tolerance was significantly improved by weight loss in mice administered vehicle or PCB-77 (week 16 *versus* 12; Figure 3A; $P < 0.05$). Insulin tolerance was also significantly improved by weight loss in mice administered vehicle (week 16 *versus* 12; Figure 3B; $P < 0.05$). However, mice administered PCB-77 exhibited impaired glucose (Figure 3A; $P < 0.05$) and insulin tolerance (Figure 3B; $P < 0.05$) during the weight loss phase compared to controls. Weight loss resulted in a significant decrease in TNF- α mRNA abundance in adipose from mice administered vehicle or PCB-77 (Supplemental Material, Figure S8; $P < 0.05$). However, mice administered PCB-77 had significantly increased TNF- α mRNA abundance in adipose during weight loss compared to controls (Supplemental Material, Figure S8; $P < 0.05$).

PCB-77 results in an AhR-dependent increase in expression of TNF- α in 3T3-L1 adipocytes.

Previous studies demonstrated that the AhR ligand, PCB-77, increased mRNA abundance of TNF- α in 3T3-L1 adipocytes (Arsenescu et al. 2008). TNF- α is an intermediate in ROS generated by 2,3,7,8-tetrachloro-dibenzo-p-dioxin (TCDD), an AhR ligand (Alsharif et al. 1994). To define mechanisms for effects of coplanar PCBs to promote glucose and insulin intolerance,

we examined effects of PCB-77 on TNF- α expression in 3T3-L1 adipocytes. Moreover, to determine if effects of PCB-77 are AhR-mediated, we incubated cells with an AhR antagonist, α -NF. Incubation of differentiated 3T3-L1 adipocytes with PCB-77 significantly increased CYP1A1 mRNA abundance, indicative of AhR activation (Supplemental Material, Figure S9A; $P < 0.05$), which was abolished by α -NF. Similarly, PCB-77-induced increases in TNF- α mRNA abundance were abolished by α -NF in 3T3-L1 adipocytes (Supplemental Material, Figure S9B; $P < 0.05$).

Discussion

Results from this study demonstrate that coplanar PCBs induce rapid and sustained glucose and insulin intolerance in lean mice in an AhR-dependent manner. These effects were associated with pronounced accumulation of PCB to adipose, most likely contributing to adipose-specific increases in expression of TNF- α . Remarkably, when mice were made obese from consumption of a HF diet and exposed to PCBs, harmful effects of the toxin to promote glucose and insulin intolerance were lost. However, when obese mice previously exposed to PCB lost weight, impairment of glucose and insulin tolerance became evident and mitigated beneficial effects of weight loss to improve glucose homeostasis. Moreover, adipose expression levels of TNF- α , while not influenced by PCB-77 during the weight gain phase of HF feeding, were increased upon weight loss. In cultured adipocytes, PCB-77 promoted TNF- α expression through an AhR-dependent mechanism. These results suggest that PCBs could promote insulin resistance through adipose-specific increases in TNF- α . Moreover, these results suggest that a greater body burden of PCBs with obesity concentrates the toxin to adipose tissue, resulting in

increased adipose TNF- α expression and insulin resistance upon liberation of PCBs during weight loss.

Increasing evidence suggests that background exposure to persistent organic pollutants is linked to the development of T2D. US Air Force veterans of the Vietnam War who were exposed to Agent Orange contaminated with dioxin had increased risk of diabetes, reduced time-to-onset of disease, and increased diabetes severity (Henriksen et al. 1997). In a cross sectional study among the general population of Japan covering the years of 2002-2006, blood levels representing the highest quartiles of PCB-126 and PCB-105 had adjusted odds ratios of 9.1 and 7.3, respectively (Uemura et al. 2009). Recent results from the Anniston Community Health Survey demonstrated significant associations between elevated PCB levels and diabetes (Silverstone et al. 2012). Serum levels of PCB-77 in the present study ($\approx 3 \mu\text{M}$) were similar to levels (1.43 ppb, equivalent to $\approx 5 \mu\text{M}$) observed in the lowest quartile of subjects from the Anniston Community (Silverstone et al. 2012). Our results demonstrate that lean mice respond to coplanar PCBs with impaired glucose and insulin tolerance, supporting an interaction between PCB exposures and the development of insulin resistance. We used this mouse model of PCB-induced glucose and insulin intolerance to define mechanisms linking PCB exposures to dysregulated glucose homeostasis.

In this study we demonstrated that PCB-77, an abundant coplanar PCB in the environment (McFarland and Clarke 1989), as well as PCB-126, a coplanar PCB that has been linked to diabetes (Everett et al. 2007), both resulted in dose-dependent rapid impairment of glucose and insulin tolerance in lean mice. Interestingly, mice exposed to the highest dose of

either PCB did not have impaired glucose or insulin tolerance; however, these mice demonstrated abnormal behavior (lethargy, tremors), polyuria, and gained minimal weight suggesting that higher doses of PCB had deleterious health consequences. Recent studies demonstrated that consumption of farmed salmon containing persistent organic pollutants, including increased levels of 7 different PCBs, promoted glucose intolerance associated with elevations in adipose tissue expression of TNF- α in HF-fed mice (Ibrahim et al. 2011). Interestingly, when levels of pollutants were decreased by feeding farm raised salmon purified fish oil, glucose tolerance improved and adipose expression levels of TNF- α decreased. Our results are in agreement with these findings, and extend these studies by demonstrating that individual coplanar PCBs promote glucose and insulin intolerance associated with adipose-specific elevations in expression of TNF- α . Moreover, similar to previous findings (Ibrahim et al. 2011), adipose contained markedly higher PCB levels compared to liver and serum, suggesting that chronic exposures of adipocytes to PCBs most likely contributed to selective increases in TNF- α expression in adipose, but not in liver or muscle.

Previous studies in our laboratory demonstrated that coplanar PCBs increased mRNA abundance of TNF- α in cultured adipocytes (Arsenescu et al. 2008). Results from this study demonstrate that PCB-77-induced increases in TNF- α expression are AhR-mediated. Moreover, concentrations (3.4 μ M) of PCB-77 used in *in vitro* studies with cultured adipocytes were comparable to serum levels (3 μ M) of PCB-77 that induced glucose and insulin intolerance in mice. Recent studies demonstrated that exposures of 3T3-L1 adipocytes to dioxin increased mRNA abundance of several proinflammatory factors, including TNF- α receptors (Kim et al. 2012). When dioxin was administered to mice fed standard mouse diet, mRNA abundance of

TNF- α in adipose tissue was markedly increased, and this effect was abolished in AhR deficient mice. Our results confirm and extend previous studies by demonstrating that *in vivo* effects of PCB-77 to impair glucose homeostasis are AhR-mediated. An interesting finding of this study was that levels of PCB-77 in adipose tissue were markedly decreased at 4 weeks after the last dose; however, mice continued to exhibit glucose and insulin intolerance. PCB-induced activation of AhR induces gene expression of CYP1A1, which hydroxylates the toxin to increase water solubility for elimination. Rapid declines in levels of PCB-77, in the face of sustained impairment of glucose homeostasis, suggest that metabolites of PCB-77 may have contributed to long-lasting impairment of glucose and insulin intolerance in mice.

In this study, while PCB-77 impaired glucose and insulin tolerance in lean mice, these effects were lost when mice were fed a HF diet. The lipophilic nature of PCBs results in their accumulation in adipocyte lipid-containing droplets. For example, in humans, body mass index is inversely correlated with serum levels of PCBs, supporting the concept that an expanded adipose mass results in redistribution of PCBs away from the circulating compartment (Dirinck et al. 2011). In support, recent studies demonstrated increased (2.9-fold) total body burden of PCBs in obese subjects (Kim et al. 2011). Thus, sequestration of PCB-77 in adipocyte lipid pools as demonstrated by higher levels in adipose tissue from HF-fed mice in this study most likely resulted in restricted access to AhR, contributing to a lack of effect of PCB-77 on glucose and/or insulin tolerance in obese mice. Alternatively, effects of PCB-77 to impair glucose homeostasis may have become apparent with longer durations of HF-feeding. Previous studies demonstrated that plasma levels of 13 out of 17 measured organochlorines in human serum

increased with weight loss (Pelletier et al. 2002). Similarly, obese subjects experiencing drastic weight loss from bariatric surgery had increased serum levels of PCBs, which decreased the beneficial effects of weight loss (Kim et al. 2011). In agreement with previous findings, our results demonstrate that beneficial effects of weight loss to improve glucose and insulin tolerance in mice were blunted in mice administered PCB-77. Moreover, our results extend previous findings by demonstrating that adipose elevations in TNF- α may have contributed to impaired glucose and insulin tolerance in PCB-exposed mice experiencing weight loss.

In conclusion, results from this study demonstrate that coplanar PCBs cause rapid and sustained impairment of glucose and insulin tolerance in mice through an AhR-dependent mechanism associated with an adipose-specific increase in expression levels of TNF- α . While harmful effects of PCB-77 on glucose and insulin tolerance were absent in obese mice, beneficial effects of weight loss to improve glucose and insulin tolerance were mitigated in mice previously exposed to PCB-77. These results suggest that sequestration of lipophilic coplanar PCBs to adipose may contribute to AhR-mediated increases in TNF- α and the development of adipocyte insulin resistance, an effect manifest in lean conditions as well as during weight loss when adipose-derived toxins may be liberated.

References

- Alsharif NZ, Lawson T, Stohs SJ. 1994. Oxidative stress induced by 2,3,7,8-tetrachlorodibenzo-p-dioxin is mediated by the aryl hydrocarbon (Ah) receptor complex. *Toxicology* 92(1-3):39-51.
- Arsenescu V, Arsenescu RI, King V, Swanson H, Cassis LA. 2008. Polychlorinated biphenyl-77 induces adipocyte differentiation and proinflammatory adipokines and promotes obesity and atherosclerosis. *Environ Health Perspect* 116(6):761-768.
- Cardoso FC, Sears W, LeBlanc SJ, Drackley JK. 2011. Technical note: comparison of 3 methods for analyzing areas under the curve for glucose and nonesterified fatty acids concentrations following epinephrine challenge in dairy cows. *J Dairy Sci* 94(12):6111-6115.
- Carpenter DO. 2008. Environmental contaminants as risk factors for developing diabetes. *Rev Environ Health* 23(1):59-74.
- Cawthorn WP, Sethi JK. 2008. TNF-alpha and adipocyte biology. *FEBS Lett* 582(1):117-131.
- Chevrier J, Dewailly E, Ayotte P, Mauriege P, Despres JP, Tremblay A. 2000. Body weight loss increases plasma and adipose tissue concentrations of potentially toxic pollutants in obese individuals. *Int J Obes Relat Metab Disord* 24(10):1272-1278.
- Choi EY, Lee H, Dingle RW, Kim KB, Swanson HI. 2012. Development of novel CH223191-based antagonists of the aryl hydrocarbon receptor. *Mol Pharmacol* 81(1):3-11.
- Codru N, Schymura MJ, Negoita S, Rej R, Carpenter DO. 2007. Diabetes in relation to serum levels of polychlorinated biphenyls and chlorinated pesticides in adult Native Americans. *Environ Health Perspect* 115(10):1442-1447.
- DeFronzo RA. 2004. Pathogenesis of type 2 diabetes mellitus. *Med Clin North Am* 88(4):787-835, ix.
- Denison MS, Nagy SR. 2003. Activation of the aryl hydrocarbon receptor by structurally diverse exogenous and endogenous chemicals. *Annu Rev Pharmacol Toxicol* 43:309-334.
- Dirinck E, Jorens PG, Covaci A, Geens T, Roosens L, Neels H, et al. 2011. Obesity and persistent organic pollutants: possible obesogenic effect of organochlorine pesticides and polychlorinated biphenyls. *Obesity (Silver Spring)* 19(4):709-714.
- Everett CJ, Frithsen IL, Diaz VA, Koopman RJ, Simpson WM, Jr., Mainous AG, 3rd. 2007. Association of a polychlorinated dibenzo-p-dioxin, a polychlorinated biphenyl, and DDT

- with diabetes in the 1999-2002 National Health and Nutrition Examination Survey. *Environ Res* 103(3):413-418.
- Hansen LG. 1998. Stepping backward to improve assessment of PCB congener toxicities. *Environ Health Perspect* 106(1):171-189.
- Harford KA, Reynolds CM, McGillicuddy FC, Roche HM. 2011. Fats, inflammation and insulin resistance: insights to the role of macrophage and T-cell accumulation in adipose tissue. *Proc Nutr Soc* 70(4):408-417.
- Henriksen GL, Ketchum NS, Michalek JE, Swaby JA. 1997. Serum dioxin and diabetes mellitus in veterans of Operation Ranch Hand. *Epidemiology* 8(3):252-258.
- Hotamisligil GS, Peraldi P, Budavari A, Ellis R, White MF, Spiegelman BM. 1996. IRS-1-mediated inhibition of insulin receptor tyrosine kinase activity in TNF- α - and obesity-induced insulin resistance. *Science* 271(5249):665-668.
- Ibrahim MM, Fjaere E, Lock EJ, Naville D, Amlund H, Meugnier E, et al. 2011. Chronic consumption of farmed salmon containing persistent organic pollutants causes insulin resistance and obesity in mice. *PLoS One* 6(9):e25170.
- Kienesberger PC, Lee D, Puliniilkunnil T, Brenner DS, Cai L, Magnes C, et al. 2009. Adipose triglyceride lipase deficiency causes tissue-specific changes in insulin signaling. *J Biol Chem* 284(44):30218-30229.
- Kim MJ, Marchand P, Henegar C, Antignac JP, Alili R, Poitou C, et al. 2011. Fate and complex pathogenic effects of dioxins and polychlorinated biphenyls in obese subjects before and after drastic weight loss. *Environ Health Perspect* 119(3):377-383.
- Kim MJ, Pelloux V, Guyot E, Tordjman J, Bui LC, Chevallier A, et al. 2012. Inflammatory pathway genes belong to major targets of persistent organic pollutants in adipose cells. *Environ Health Perspect* 120(4):508-514.
- Kim SH, Henry EC, Kim DK, Kim YH, Shin KJ, Han MS, et al. 2006. Novel compound 2-methyl-2H-pyrazole-3-carboxylic acid (2-methyl-4-o-tolylazo-phenyl)-amide (CH-223191) prevents 2,3,7,8-TCDD-induced toxicity by antagonizing the aryl hydrocarbon receptor. *Mol Pharmacol* 69(6):1871-8.
- Kodavanti PR, Ward TR, Derr-Yellin EC, Mundy WR, Casey AC, Bush B, et al. 1998. Congener-specific distribution of polychlorinated biphenyls in brain regions, blood, liver,

- and fat of adult rats following repeated exposure to Aroclor 1254. *Toxicol Appl Pharmacol* 153(2):199-210.
- Lee DH, Steffes MW, Sjodin A, Jones RS, Needham LL, Jacobs DR, Jr. 2010. Low dose of some persistent organic pollutants predicts type 2 diabetes: a nested case-control study. *Environ Health Perspect* 118(9):1235-1242.
- Lim JS, Son HK, Park SK, Jacobs DR, Jr., Lee DH. 2011. Inverse associations between long-term weight change and serum concentrations of persistent organic pollutants. *Int J Obes (Lond)* 35(5):744-747.
- McFarland VA, Clarke JU. 1989. Environmental occurrence, abundance, and potential toxicity of polychlorinated biphenyl congeners: considerations for a congener-specific analysis. *Environ Health Perspect* 81:225-239.
- Patel CJ, Bhattacharya J, Butte AJ. 2010. An Environment-Wide Association Study (EWAS) on type 2 diabetes mellitus. *PLoS One* 5(5):e10746.
- Pelletier C, Doucet E, Imbeault P, Tremblay A. 2002. Associations between weight loss-induced changes in plasma organochlorine concentrations, serum T(3) concentration, and resting metabolic rate. *Toxicol Sci* 67(1):46-51.
- Peraldi P, Hotamisligil GS, Buurman WA, White MF, Spiegelman BM. 1996. Tumor necrosis factor (TNF)-alpha inhibits insulin signaling through stimulation of the p55 TNF receptor and activation of sphingomyelinase. *J Biol Chem* 271(22):13018-13022.
- Peraldi P, Spiegelman B. 1998. TNF-alpha and insulin resistance: summary and future prospects. *Mol Cell Biochem* 182(1-2):169-175.
- Shaw JE, Sicree RA, Zimmet PZ. 2010. Global estimates of the prevalence of diabetes for 2010 and 2030. *Diabetes Res Clin Pract* 87(1):4-14.
- Silverstone AE, Rosenbaum PF, Weinstock RS, Bartell SM, Foushee HR, Shelton C, et al. 2012. Polychlorinated Biphenyl (PCB) Exposure and Diabetes: Results from the Anniston Community Health Survey. *Environ Health Perspect*. 120(5):727-732.
- Thong FS, Dugani CB, Klip A. 2005. Turning signals on and off: GLUT4 traffic in the insulin-signaling highway. *Physiology (Bethesda)* 20:271-284.
- Torti FM, Torti SV, Larrick JW, Ringold GM. 1989. Modulation of adipocyte differentiation by tumor necrosis factor and transforming growth factor beta. *J Cell Biol* 108(3):1105-1113.

- Uemura H, Arisawa K, Hiyoshi M, Kitayama A, Takami H, Sawachika F, et al. 2009. Prevalence of metabolic syndrome associated with body burden levels of dioxin and related compounds among Japan's general population. *Environ Health Perspect* 117(4):568-573.
- Ventre J, Doebber T, Wu M, MacNaul K, Stevens K, Pasparakis M, et al. 1997. Targeted disruption of the tumor necrosis factor-alpha gene: metabolic consequences in obese and nonobese mice. *Diabetes* 46(9):1526-1531.
- Walford RL, Mock D, MacCallum T, Laseter JL. 1999. Physiologic changes in humans subjected to severe, selective calorie restriction for two years in biosphere 2: health, aging, and toxicological perspectives. *Toxicol Sci* 52(2 Suppl):61-65.
- Wang SL, Tsai PC, Yang CY, Leon Guo Y. 2008. Increased risk of diabetes and polychlorinated biphenyls and dioxins: a 24-year follow-up study of the Yucheng cohort. *Diabetes Care* 31(8):1574-1579.

Figure Legends

Figure 1. PCB-77 (A) and PCB-126 (B) impair glucose tolerance in LF-fed mice. (A), Blood glucose concentrations following a bolus of glucose in mice administered vehicle (VEH), 2.5, 50 or 248 mg/kg of PCB-77 (48 hours after the second dose). (B), Blood glucose concentrations following a bolus of glucose in mice administered vehicle, 0.3, 1.6 or 3.3 mg/kg of PCB-126 (48 hours after the second dose). Data are mean \pm SEM from $n = 5$ mice/dose of PCB. *, $P < 0.05$ compared to VEH within a time point. (C,D), Quantification of total area under the curve (AUC) for data in A, B, respectively. *, $P < 0.05$ compared to VEH.

Figure 2. PCB-77 results in elevated TNF- α expression in adipose, but not in liver or soleus muscle of LF-fed mice. Mice were administered vehicle (VEH) or PCB-77 (50 mg/kg, 2 doses) and expression levels of TNF- α quantified in adipose, liver or soleus muscle 2 weeks later (week 4). Data are mean \pm SEM from $n = 3$ mice/group. *, $P < 0.05$ compared to VEH.

Figure 3. PCB-77 has no effect on glucose (A) or insulin (B) tolerance in HF-fed mice during weight gain, but impairs glucose homeostasis during weight loss. (A), Total area under the curve (AUC) for glucose tolerance in mice administered vehicle (VEH) or PCB-77 (50 mg/kg, 2 doses during weeks 1 and 2 and a second 2 doses during weeks 9 and 10) during weight gain (weeks 4, 12 of HF feeding) or weight loss (at week 16 after mice are switched to a LF diet). Data are mean \pm SEM from $n \geq 5$ mice/group. *, $P < 0.05$ compared to week 12 within treatment group. **, $P < 0.05$ compared to VEH within time point.

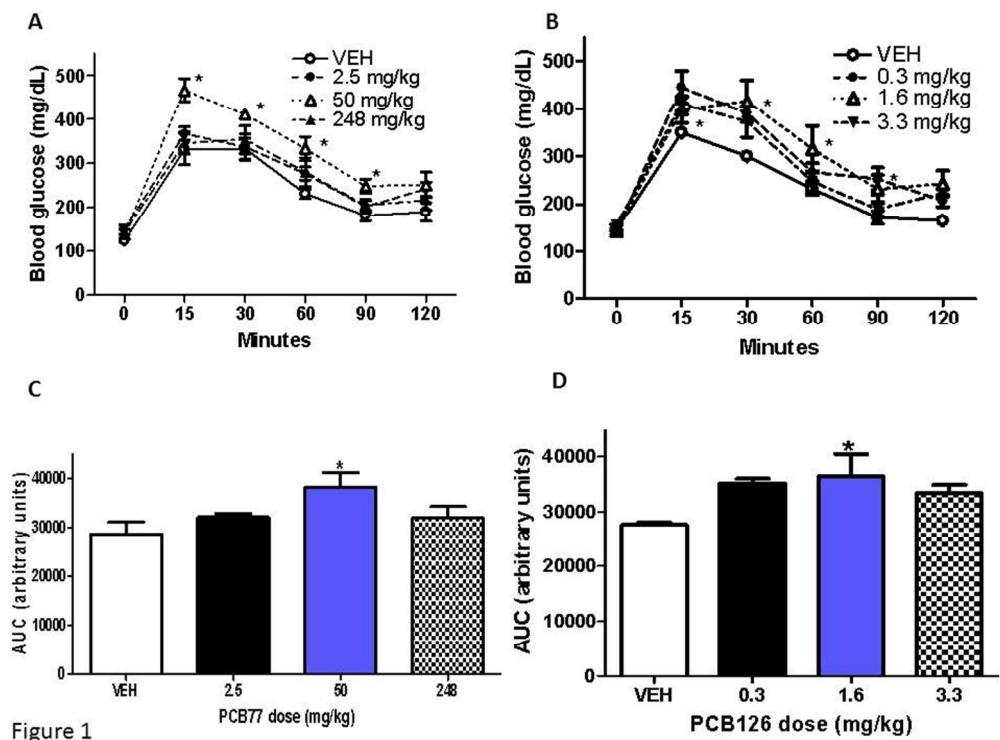


Figure 1

Figure 1
254x190mm (96 x 96 DPI)

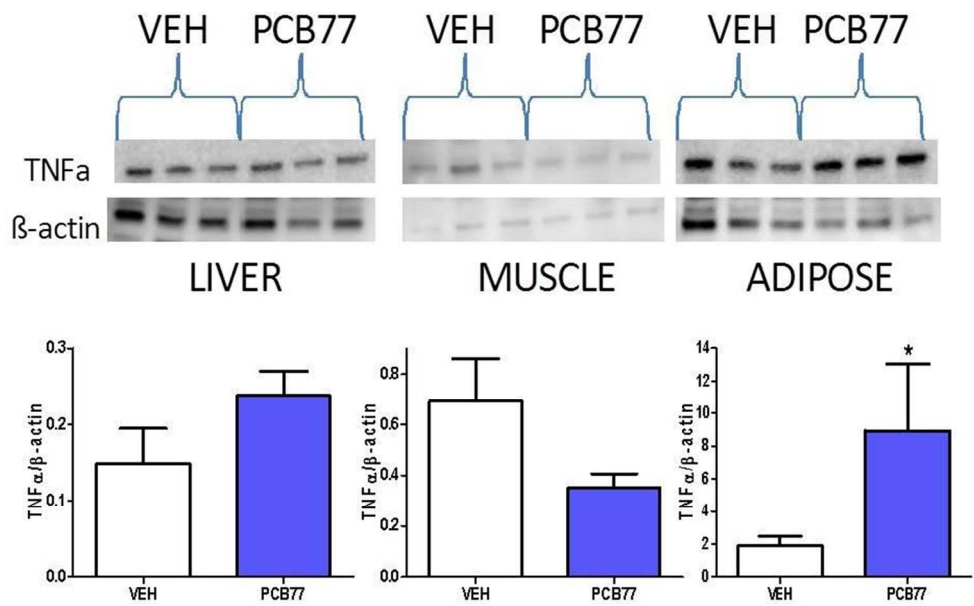


Figure 2

Figure 2
254x190mm (96 x 96 DPI)

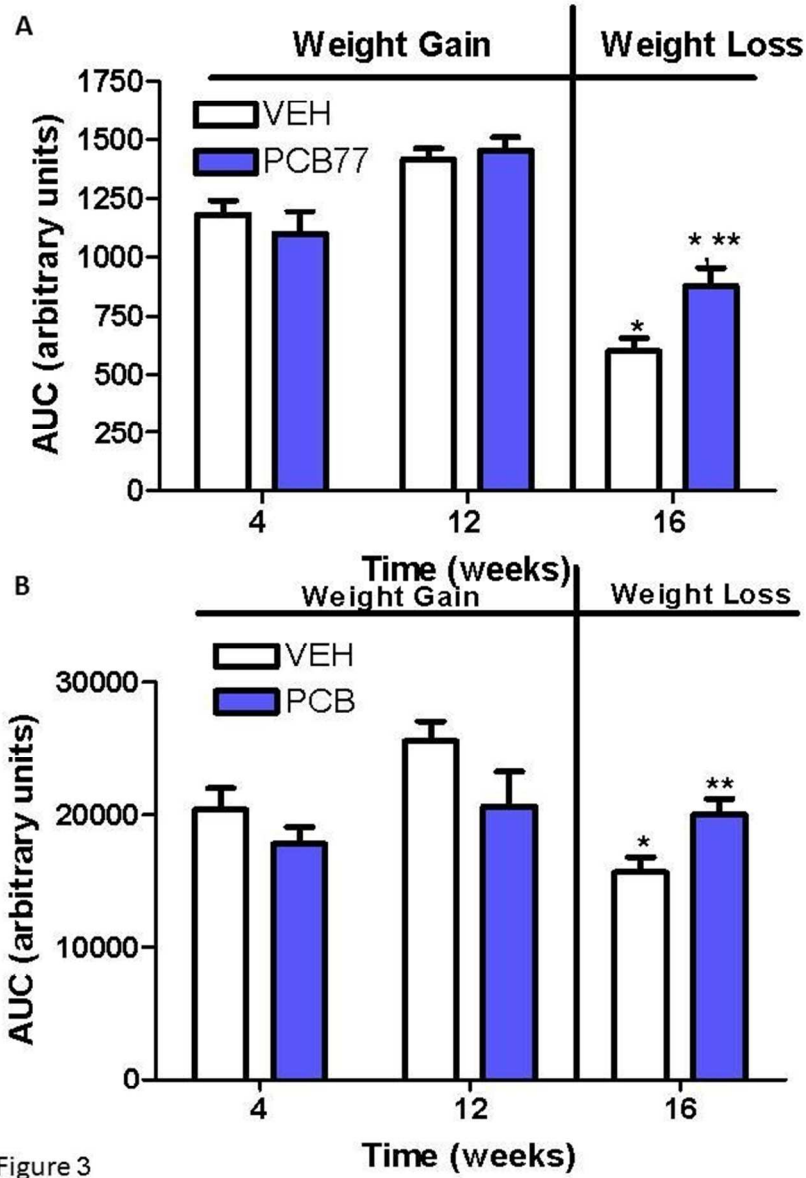


Figure 3

Figure 3
190x254mm (96 x 96 DPI)